Carbohydrate Polymers 87 (2012) 1185–1191

Contents lists available at SciVerse ScienceDirect

Carbohydrate Polymers

journal homepage: www.elsevier.com/locate/carbpol

# Magnetic chitosan composite particles: Evaluation of thorium and uranyl ion adsorption from aqueous solutions

Doina Hritcu [a,*], Doina Humelnicu [b,*], Gianina Dodi [a], Marcel Ionel Popa [a]

[a] Faculty of Chemical Engineering and Environmental Protection, "Gheorghe Asachi" Technical University of Iasi, 73, Bd. Prof. dr. docent Dimitrie Mangeron, 700050 Iasi, Romania
[b] "Al.I.Cuza" University of Iasi, Faculty of Chemistry, 11, Carol I Bd., 700506 Iasi, Romania

ARTICLE INFO

*Article history:*
Received 25 May 2011
Received in revised form 29 August 2011
Accepted 30 August 2011
Available online 6 September 2011

*Keywords:*
Magnetic adsorbent
Chitosan composite particle
Thorium ion
Uranyl ion
Adsorption

ABSTRACT

Magnetic chitosan composite particles with 40 μm average size and 24 emu/g saturation magnetization obtained by an in situ procedure were evaluated as a new low-cost adsorbent for radioactive wastewater decontamination. Sorbent characterization by SEM, EDX, FTIR and magnetization measurements proved that the target ions were bound and their surface distribution was uniform. The 18 emu/g magnetization of the metal loaded particles was high enough to ensure their easy magnetic field separation and recovery. The parameters influencing the sorption process were optimized with respect to sorbent mass, target ion concentration and contact time. The material under study had superior adsorption capacity both for uranyl (666.67 mg/g) and thorium (312.50 mg/g) ions when compared to other low-cost adsorbents reported in literature. The adsorption process is spontaneous and endothermic. The material may be regenerated and re-used.



## 1. Introduction

Significant research efforts are currently directed towards removing radioactive ions such as thorium, uranium and other actinides from residual waters due to their high toxicity and potential harm to the environment (Talip, Eral, & Hicsönmez, 2009). Comprehensive knowledge of the behavior of wastewaters has been used to develop various processes for their decontamination treatment such as: chemical precipitation, membrane separation, ion exchange, electrodialysis, photocatalysis and adsorption procedures (Barakat, in press). Adsorption is by far the easiest way for removing radioactive ions from aqueous solutions. Various types of materials have been used for thorium and uranyl sorption, for example activated carbon powder and zeolites (Kutahyali & Eral, 2010), immobilized siloxane polymers (Akperov, Maharramov, & Akperov, 2009), natural and modified clays (Guerra, Viana, & Airoldi, 2009), synthetic anion exchangers (Korichia & Bensmailia, 2009) etc.

In the field of water treatment, especially in the removal of heavy metals, natural polymers, mainly polysaccharides, have shown excellent potential, due to their low cost, availability and advantageous presence of hydroxyl, amino and other active functional groups on the backbone chain (Crini, 2005). A comprehensive review of recent literature presented by Muzzarelli (2011) evidences the significant role that chitin/chitosan containing materials is expected to play in uranium separation from seawater.

Natural polymers present however some disadvantages that limit their use in practical wastewater treatment applications, such as their weak mechanical properties, poor chemical resistance, low surface area and difficult separation from the liquid phase. Magnetic sorbents on the other hand, especially when used in particulate form, have a relatively high surface area and are easy to separate and recover in magnetic field. Their advantages prevail over the difficulties normally associated with other powdered adsorbents (Ambashta & Sillanpaa, 2010). A step further in developing adsorbents with superior properties would be the inclusion of magnetic particles into natural polymers, thus combining the advantages of both materials.

Various types of magnetic particles have recently been synthesized and used as adsorbents for actinide removal, as reviewed by Rojo et al. (2009). Aamrani et al. (2007) used magnetite for the adsorption of uranyl ions and recently, Wang, Peng, Yang, Liu, & Hu (2011) studied the adsorption of uranyl ions from aqueous solutions onto ethylenediamine-modified magnetic chitosan.

The purpose of the present study is to evaluate the magnetic composite chitosan particles obtained in previously reported work by our group as a new adsorbent material for wastewater treatment. The study also aims to investigate the influence of various experimental parameters on thorium and uranyl adsorption and to

* Corresponding authors.
*E-mail addresses:* dhritcu@ch.tuiasi.ro (D. Hritcu), doinah@uaic.ro (D. Humelnicu).

0144-8617/$ – see front matter © 2011 Elsevier Ltd. All rights reserved.
doi:10.1016/j.carbpol.2011.08.095

determine the optimum procedure for the separation of radioactive ions from simulated wastewater solutions by adsorption on this new material.

## 2. Materials and methods

### 2.1. Materials

Analytical grade chemicals were used throughout this study. Magnetic iron chitosan composite particles were synthesized in our laboratory and used as a new adsorbent material. Stock solutions containing $Th^{4+}$ or $UO_2^{2+}$ ions were prepared by dissolving $Th(NO_3)_4{\cdot}4H_2O$ or $UO_2(NO_3)_2{\cdot}6H_2O$ (Merck, Germany) in distilled water.

### 2.2. Preparation of magnetic chitosan composite particles

Magnetic iron chitosan composite particles were obtained by a previously reported (Hritcu, Dodi, Silion, Popa, & Popa, 2011) in situ procedure. In a typical synthesis, the magnetic material was produced by oxidation of the ferrous ions that were already entrapped in chitosan–Fe(II) complex, using nitrate ions as a mild oxidizing agent, under alkaline conditions. The chitosan matrix was then crosslinked by addition of an aqueous glutaraldehyde solution under mechanical stirring. The cleaning procedure involved multiple aqueous washes and an acid–base treatment followed by a 3 day dialysis step against distilled water. The composite particles used in this study (synthesis lot denoted Fe–Cc) had an average diameter of 40 μm and a saturation magnetization of 24 emu/g (corresponding to an estimated magnetic material content of about 47% by weight).

### 2.3. Sorption experiments

Batch experiments were conducted for evaluating the extent of $Th^{4+}$ and $UO_2^{2+}$ ion adsorption on Fe–Cc. In order to optimize the radioactive ion removal conditions, the effect of contact time, initial ion concentration, adsorbent dosage and temperature were studied. In a typical experiment a certain amount of dry adsorbent material (0.001–0.005 g) was suspended in a 20 mL aliquot of metal ion solution with a concentration of 10–100 mg/L and placed in a stoppered glass flask. The mixture was allowed to react for a time interval varying from 30 to 210 min while keeping the temperature constant at certain values in the range of 298.15–328.15 K. The pH value was maintained constant at 5.5 in the experiments involving $Th^{4+}$ ion and respectively at 4.0 in the experiments with $UO_2^{2+}$ ion, as already optimized in previous studies (Humelnicu, Dinu, & Dragan, 2011). Following the adsorption procedure, the Fe–Cc material was separated by filtration and the residual concentration of the radioactive ions left in the supernatant phase was determined using a spectrophotometric method that involves the Arsenazo III reagent (Savyvin, 1961).

The absorbance of the complex formed between the target ion and the Arsenazo III reagent in solution has been measured spectrophotometrically at 660 nm for the thorium complex and at 650 nm respectively for the uranyl complex (Khan, Ali, & Khan, 2001; Kilincarslan & Akyil, 2005). The sorption process is described by the ion distribution coefficient, $K_d$ (mL/g), calculated using Eq. (1):

$$K_d = \frac{(C_0 - C_e)}{C_e} \times \frac{V}{m} \quad (1)$$

where $C_0$ and $C_e$ are the initial and respectively the equilibrium concentrations of the metal ion in solution (mg/L), $m$ is the mass of dry sorbent (g) and $V$ is the solution volume that was placed in contact with the sorbent (mL).

The amount of sorbed metal ion at equilibrium, $q_e$ (mg/g), was calculated from the mass balance equation:

$$q_e = \frac{(C_0 - C_e)V}{m} \quad (2)$$

where all the symbols are the same as shown above and $V$ is measured in (L).

### 2.4. Desorption experiments

The recovery of the adsorbent and its regeneration capacity are among the important factors in designing an adsorption procedure. In this study, the desorption experiments were carried out in batch system by treating the Fe–Cc material bearing adsorbed radioactive ions with 0.1 M aqueous solutions of various desorption agents such as: NaCl, $Na_2CO_3$, HCl and $HNO_3$. The material was left in contact with the desorption solution for a period of 24 h. The amount of $Th^{4+}$ or $UO_2^{2+}$ ions released into solution was monitored using the same spectrophotometric method as in the sorption experiments. The metal ion recovery percentage upon desorption from the Fe–Cc particles was calculated using the initially adsorbed metal ion amount and the amount found in solution at the end of the desorption process, according to Eq. (3):

$$\text{Recovered}\,(\%) = \frac{\text{radiocation}_{\text{ads}} - \text{radiocation}_{\text{des}}}{\text{radiocation}_{\text{ads}}} \times 100 \quad (3)$$

where $\text{radiocation}_{\text{ads}}$ is the amount of adsorbed radiocation (mg/g) and $\text{radiocation}_{\text{des}}$ is the amount of desorbed radiocation (mg/g).

### 2.5. Adsorbent characterization

The morphology of the composite particles before and after the adsorption procedures was investigated by Scanning Electron Microscope (SEM) and Energy dispersive X-ray spectrometry (Bruker AXS Microanalysis GmbH) on a dry sample. Qualitative chemical structure assessment was done by FTIR analysis (Bomem MB 104 spectrometer). The magnetic properties were measured on a VSM 7410 vibrating sample magnetometer. The concentration of the radioactive ions in solution was analyzed using a CECIL 1020 UV-vis spectrophotometer.

## 3. Results and discussions

### 3.1. Adsorbent characterization

The samples used for characterization were:

- Fe–Cc: magnetic iron chitosan composite particles before adsorption;
- Th–Fe–Cc: dry particles recovered after thorium adsorption in optimum conditions;
- U–Fe–Cc: dry particles recovered after uranyl adsorption in optimum conditions.

The SEM micrographs of the composite material before and after adsorption are shown in Fig. 1. Similar morphology features were reported for magnetic chitosan particles obtained by Wang et al. (2011). The dry surface of the polysaccharide matrix shows numerous irregularities that increase the contact area with aqueous solutions and improve metal ion adsorption.

The structure of the loaded materials after metal adsorption presented less prominent grooves.

The particles were also analyzed by EDX (Energy dispersive X-ray) before and after metal ions (uranium and thorium) adsorption. Their composition is presented in Table 1. This method is semi-quantitative.

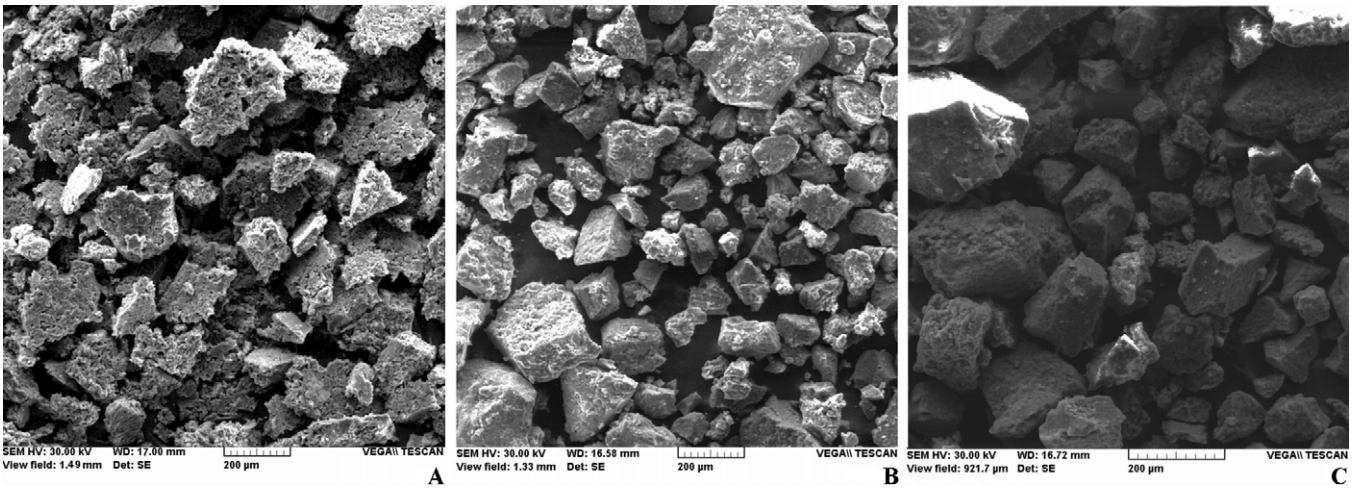


**Fig. 1.** SEM pictures of the material before (A; sample Fe–Cc) and after thorium (B; sample Th–Fe–Cc) and uranyl (C; sample U–Fe–Cc) adsorption.

The iron content (% by weight) in the Fe–Cc batch was found to be about 26.34%. This result compares well to our previously reported (Hritcu et al., 2011) estimate of its magnetic material content of about 47% as determined from the magnetization measurements. Since the magnetic core probably consists in mixed $Fe_3O_4$ and $Fe_2O_3$ oxides with an iron content of about 72 and 70% respectively, the estimated iron percentage in the composite material as calculated from magnetization is roughly 30%.

After the metal ion uptake, the EDX spectra showed new distinct peaks associated with the presence of the respective metal ions (uranium or thorium), while the iron content decreased to about 15.94% for Th–Fe–Cc and 18.81% for U–Fe–Cc sample respectively. The decrease is also confirmed by the magnetization measurements presented below in Fig. 3B. The results for the adsorbed ion content (14.64% thorium and 4.11% uranium by weight) are lower than the calculated adsorption capacities reported in Section 3.2, due to the fact that EDX method is only semi-quantitative and/or it measures the ion fraction located close to the matrix surface.

The EDX map presented in Fig. 2 provides evidence for the uniform radiocation distribution when adsorbed on the particle surface.

Comparative IR spectra of Fe–Cc, Th–Fe–Cc, and U–Fe–Cc materials are shown in Fig. 3A. Following $UO_2^{2+}$ and $Th^{4+}$ ion sorption, the spectra exhibited changes in peak positions that further indicate the radionuclide binding. The peak at 3433 $cm^{-1}$ corresponding to the stretching vibration of OH-group shifts to 3422 $cm^{-1}$ after radiocation sorption, indicating that the –OH group takes part in the sorption process. This conclusion is in agreement with other studies (Roonasi & Holmgren, 2009). The peak at 1637 $cm^{-1}$ corresponding to the vibration of $NH_2$ in amine (belonging to the chitosan matrix) shifts to 1645 $cm^{-1}$ for batch Th–Fe–Cc and respectively to 1649 $cm^{-1}$ for batch U–Fe–Cc indicating that $NH_2$ took part in the adsorption process. The strong absorption peaks located between 1027 and 1070 $cm^{-1}$ are characteristic for thorium and uranyl ions. After $Th^{4+}$ ions sorption a new band characteristic for the association of these ions with the hydroxyl groups belonging to the polysaccharide matrix appears at 1392 $cm^{-1}$ (Anirudhan, Rijith, & Tharun, 2010). An obvious change in the peak position and its intensity in the 900–400 $cm^{-1}$ region may be due to the formation of new (M–O) and (O–M–O) bonds (M = U or Th ion) (Merroun, Geipel, Nicolai, Heise, & Selenska-Pobell, 2003). In the uranium loaded sample, the distinct new peak at 900 $cm^{-1}$ and the changes in peak positions and their intensity in the 400–500 $cm^{-1}$ region may be assigned to asymmetric stretching vibration of $UO_2^{2+}$ and stretching vibrations of weakly bonded oxygen ligands with uranium ($U–O_{ligand}$) (Kazya, D'Souzab, & Sar, 2009).

Magnetic measurements were performed on dried particles before and after radioactive ions adsorption. Comparative results presented in Fig. 3B confirm that the target ions were bound to the surface causing a decrease in the magnetic material content and consequently in the measured magnetization value (from 24 to 18 emu/g).

### 3.2. Uranyl and thorium ions adsorption

#### 3.2.1. Effect of sorbent mass

In order to determine the optimum sorbent amount, experimental data regarding the variation of the distribution coefficient versus the sorbent mass were collected for both ions. In these experiments, target ion solutions with a concentration of 50 mg/L were placed in contact with various amounts of sorbent (0.001–0.005 g) for 120 min at 298.15 K. The results are presented in Fig. 4A. The adsorption of both ions increased with increasing the sorbent mass due to the availability of a higher number of adsorbing active sites. The increase slows down beyond 0.004 g sorbent for both ions.

**Table 1**
EDX analysis results.

| Element | Fe–Cc | | Th–Fe–Cc | | U–Fe–Cc | |
|---|---|---|---|---|---|---|
| | Atomic % | Wt. % | Atomic % | Wt. % | Atomic % | Wt. % |
| Oxygen | 67.41 | 57.52 | 67.83 | 54.27 | 69.94 | 60.81 |
| Iron | 8.84 | 26.34 | 5.70 | 15.94 | 6.20 | 18.81 |
| Carbon | 15.09 | 9.67 | 25.19 | 15.13 | 15.34 | 10.01 |
| Nitrogen | 8.64 | 6.45 | - | - | 8.18 | 6.23 |
| Th | – | – | 1.26 | 14.64 | – | – |
| U | – | – | – | – | 0.31 | 4.11 |

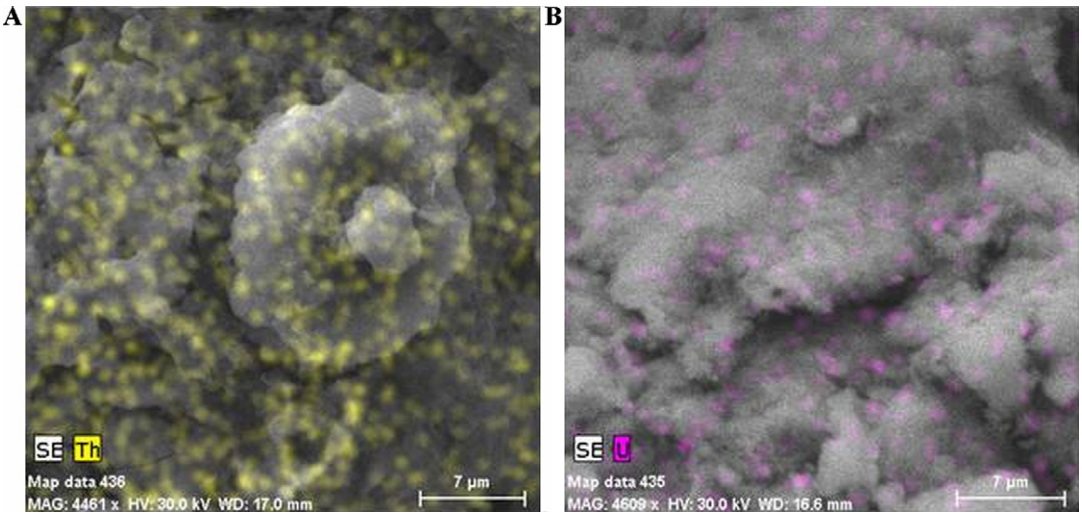


**Fig. 2.** EDX map showing uniform distribution of the thorium (A) and uranyl (B) ions onto the composite particle surface.

*3.2.2. Effect of contact time*

In order to determine the optimum contact time, its value was varied in the range of 30–210 min in a series of experiments in which the initial target ion concentration, the temperature and the adsorbent amount were kept constant at 50 mg/L, 298.15 K and 0.004 g respectively. The data regarding the distribution coefficient variation versus the contact time are presented in Fig. 4B. The adsorption equilibrium is reached after 120 min for both ions. Further increase in contact time does not affect the adsorption process.

*3.2.3. Effect of initial metal ion concentration*

In order to determine the optimum initial concentration of the target ion, its value was varied (for both ions under study) in the range of 10–100 mg/L, while keeping the temperature, the sorbent mass and the contact time constant at 298.15 K, 0.004 g and 120 min respectively. The data regarding the variation of the distribution coefficient versus the initial metal ion concentration are presented in Fig. 4C. The adsorption capacity of the Fe–Cc material decreases with increasing the ion concentration in both cases, eventually reaching saturation.

*3.2.4. Adsorption isotherms*

The experimental data collected at 298.15 K and initial ion concentration of 50 mg/L were fitted on the standard models used in wastewater treatment applications: Langmuir, Freundlich, and respectively Dubinin–Radushkevich isotherm.

The Langmuir model assumes that the solid surface carries a limited number of sites that are characterized by equal energy of adsorption, independent of the degree of coverage and thus indicating a monolayered adsorption. The linearized form of the Langmuir equation (Akkaya & Ulusoy, 2008; Ozmen et al., 2010) is described by Eq. (4):

$$\frac{C_e}{q_e} = \frac{1}{K_L \times q_m} + \frac{C_e}{q_m} \tag{4}$$

where $C_e$ is the sorbate equilibrium concentration (mg/L), $q_e$ is the amount of solute adsorbed per mass unit of adsorbent (mg/g), $q_m$ relates to the saturated adsorption capacity (mg/g) and $K_L$ is related to the affinity of the sorbate for the adsorbent (L/mg). This model generates an "L" isotherm that reaches a plateau (Limousin et al., 2007).

The Freundlich model assumes that the adsorption surface is heterogeneous. It generates an "L" isotherm that does not reach a plateau as $C_e$ increases (Limousin et al., 2007). The linearized form of the Freundlich equation is given as,

$$\log \quad q_e = \log \quad K_F + \frac{1}{n} \quad \log \quad C_e \tag{5}$$

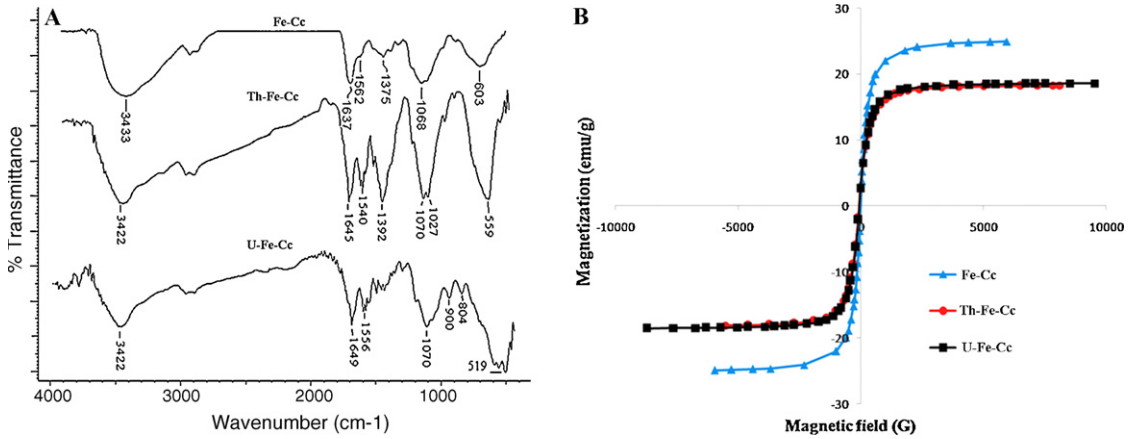


**Fig. 3.** A. IR spectra for magnetic chitosan composite before (Fe–Cc), and after the adsorption (Th–Fe–Cc, U–Fe–Cc). (B) Magnetization measurements before (Fe–Cc) and after radioactive ions adsorption (Th–Fe–Cc, U–Fe–Cc).

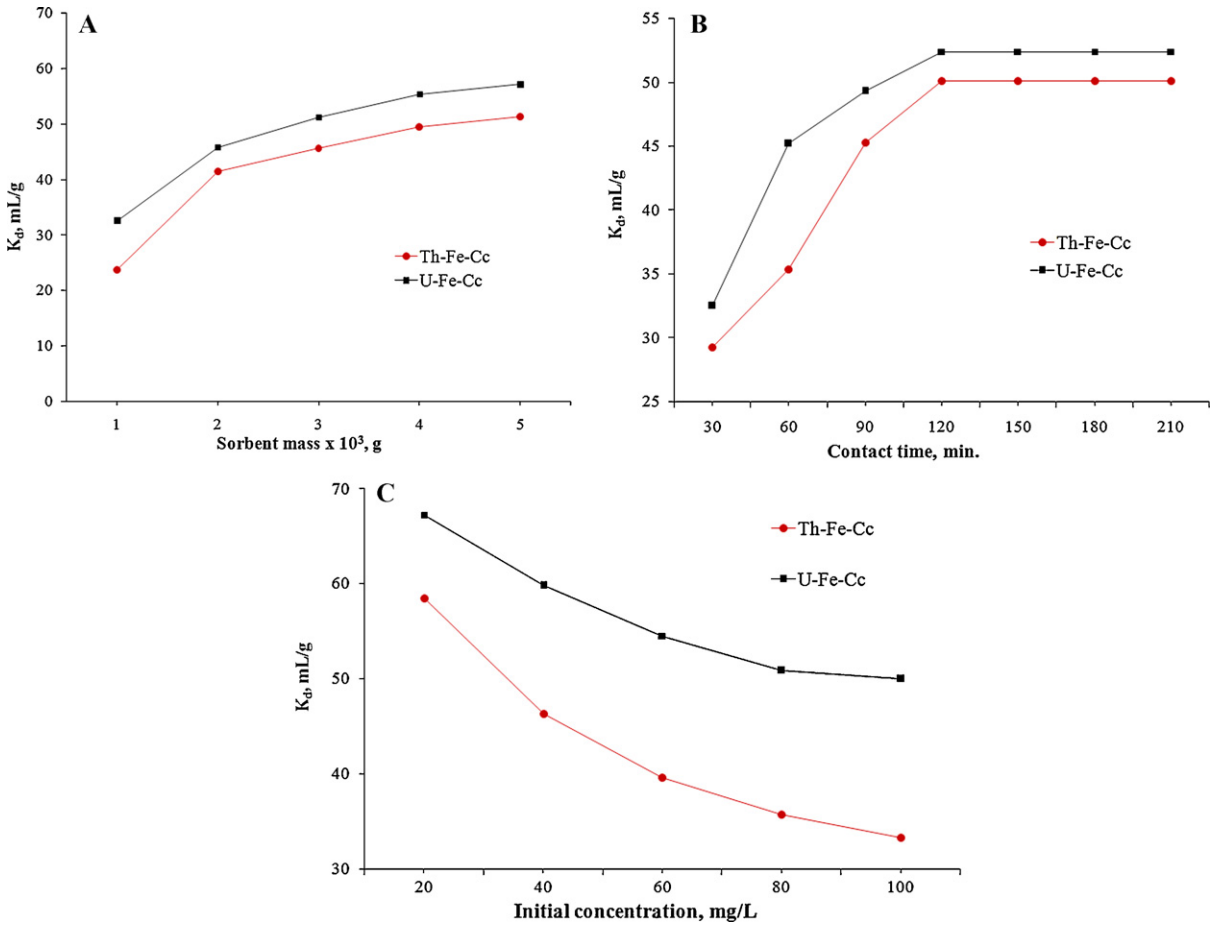


**Fig. 4.** (A) Distribution coefficient for $Th^{+4}$ and $UO_2^{2+}$ ion adsorption on Fe–Cc material as a function of sorbent mass. (B) Effect of contact time on the distribution coefficient for $Th^{+4}$ and $UO_2^{2+}$ ion adsorption on Fe–Cc material. (C) Effect of initial ion concentration on the distribution coefficient for $Th^{+4}$ and $UO_2^{2+}$ ion adsorption on Fe–Cc material.

where $K_F$ and $1/n$ are the Freundlich constants; $K_F$ represents the relative sorption capacity, and $1/n$ the intensity of the sorption process.

The linearized Dubinin–Radushkevich equation (Chen, Liu, Chen, & Chen, 2008) may be written as,

$$\ln \quad q_e = \ln \quad X_m - K_{DR}\varepsilon^2 \tag{6}$$

where $K_{DR}$ s a constant related to the adsorption energy ($mol^2/kJ^2$), $X_m$ is a constant that indicates the sorption degree characterizing the sorbent (mg/g) and $\varepsilon$ is the Polanyi potential shown in Eq. (7):

$$\varepsilon = RT \quad \ln\left(1 + \frac{1}{C_e}\right) \tag{7}$$

where $T$ is the absolute temperature (K) and $R$ is the ideal gas constant ($R = 8.314$ J/molK).

The free energy of adsorption ($E_S$) is calculated with the equation:

$$E_S = (-2K_{DR})^{-1/2} \tag{8}$$

The correlation coefficients indicate that the experimental data regarding the adsorption on the material under study is best described by the Langmuir model. The other two models were used for the characterization of the general adsorption mechanism on the material under study.

The corresponding Freundlich, Langmuir and Dubinin–Radushkevich parameters along with the correlation coefficients are reported in Table 2.

While the Freundlich and Dubinin–Radushkevich constants obtained for thorium and uranyl are similar in value ($K_F$ is 91.96 for thorium and respectively 90.01 for uranyl; $X_m$ is 91.46 for thorium and respectively 92.11 for uranyl), the constants obtained from the Langmuir isotherm are different for the two ions. The higher $q_m$ value of uranyl ions ($q_m = 666.67$ mg/g) compared with that of thorium ions ($q_m = 312.50$ mg/g) suggests that the composite particles have a superior adsorption capacity for the uranyl ions.

In order to compare the data obtained from the Langmuir plot with the magnetization measurements, the following equation was used for predicting the saturation magnetization after adsorption:

$$M_{ads} = 24 \times \frac{1}{1 + q_m \times 10^{-3}} \tag{9}$$

where $M_{ads}$ is the saturation magnetization after adsorption (emu/g), 24 is the saturation magnetization before adsorption (emu/g), 1 is initial weight of the material (g), $q_m$ is the adsorption capacity from the Langmuir plot (mg/g).

Using this equation, the predicted saturation magnetization would be of about 14 emu/g after uranyl adsorption and about 18 emu/g after thorium adsorption, evidencing good correlation between the two sets of data.

As shown in Table 2, $n = 6.188$ ($1/n = 0.161$) for thorium ions and $n = 5.98$ ($1/n = 0.167$) for uranyl ions; the data fits the requirement of the Freundlich equation (usually $0 < (1/n) < 1$).

In addition, the mean adsorption energy ($E_S$) calculated from the D–R isotherm, is useful for predicting whether the adsorption process is physical (at $E_S$ values in the range of 1–8 kJ/mol) or chemical (at $E_S$ values of more than 8 kJ/mol) in its nature (Chen & Chen, 2009). The $E_S$ values calculated from the $D$–$R$ plot indicate that the

**Table 2**
Constants obtained from the Langmuir, Freundlich and Dubinin–Radushkevich sorption isotherms at 298.15 K.

| Radioactive ion | Langmuir constants | | | Freundlich constants | | | Dubinin–Radushkevich constants | | |
|---|---|---|---|---|---|---|---|---|---|
| | $R^2$ | $q_m$ (mg/g) | $K_L$ (L/mg) | $R^2$ | $K_F$ | $n$ | $R^2$ | $X_m$ (mg/g) | $K_{DR}$ |
| $Th^{4+}$ | 0.9767 | 312.50 | 0.219 | 0.9466 | 91.96 | 6.188 | 0.9462 | 91.46 | -0.374 |
| $UO_2^{2+}$ | 0.9848 | 666.67 | 0.112 | 0.9607 | 90.01 | 5.984 | 0.9454 | 92.11 | -0.383 |

**Table 3**
Thermodynamic parameters for the sorption of $Th^{+4}$ and $UO_2^{2+}$ on Fe–Cc particles.

| Sample | $\Delta H$ (J/mol) | $\Delta S$ (J/mol K) | $\Delta G$ (kJ/mol) | | | |
|---|---|---|---|---|---|---|
| | | | 298.15 | 308.15 | 318.15 | 328.15 |
| Th–Fe–Cc | 11.14 | 68.75 | −19.05 | −19.69 | −20.33 | −20.96 |
| U–Fe–Cc | 9.31 | 63.93 | −20.48 | −21.17 | −21.86 | −22.55 |

adsorption of both ions onto the composite particles occurs mainly through physical sorption mechanisms.

The magnitude of $E_S$ (kJ/mol) in the Dubinin–Radushkevich (D–R) models is useful for evaluating the adsorption process type. In the present case, the positive values obtained for thorium ($E_S$ = 1.14 kJ/mol) and uranyl ($E_S$ = 1.16 kJ/mol) ions indicate that the adsorption is an endothermic process favoured at high temperature.

*3.2.5. Effect of temperature and thermodynamic data*

The effect of temperature on the adsorption of thorium and uranium on Fe–Cc particles has been studied in the range of 298.15–328.15 K, keeping all the other parameters constant at their optimum value, that is the sorbent mass (0.004 g), the target ion concentration (50 mg/L) and the contact time (120 min). The results show that the adsorption of both ions is favoured by an increase in temperature.

The thermodynamic parameters, namely the enthalpy ($\Delta H$) and entropy ($\Delta S$) associated with the adsorption process were calculated from the slope and intercept of the linear plot of $\ln K_d$ versus the reciprocal value of the temperature ($1/T$) using the following equation:

$$\ln \quad K_d = \frac{\Delta S}{R} - \frac{\Delta H}{RT} \tag{10}$$

where $K_d$ is the distribution coefficient. The correlation coefficient for the linear plot was $R^2$ = 0.999 for thorium and respectively $R^2$ = 0.995 for uranyl ions.

The Gibbs free energy of specific adsorption ($\Delta G$) was calculated using the equation:

$$\Delta G = \Delta H - T\Delta S \tag{11}$$

The estimated thermodynamic parameters are presented in Table 3. The fact the enthalpy is positive (11.14 J/mol for thorium and respectively 9.31 J/mol for uranyl) is consistent with an adsorption process that is favoured by an increase in temperature. The estimated enthalpy value of less than 40 kJ/mol indicates that the sorbate binding to the surface occurs mainly by physical, rather than chemical sorption.

The negative values of the free energy show that the radiocations are spontaneously adsorbed on the composite particles within the studied temperature range.

## 4. Desorption studies

The results regarding the cation recovery percentage when various desorbing agents were used are shown in Table 4.

Both radiocations may be desorbed efficiently from the sorbent, allowing it to be re-used in subsequent cycles. The maximum thorium ion desorption level from the composite particles (87%) was obtained when using the 0.1 M $HNO_3$ solution, while the 0.1 M $Na_2CO_3$ and the 0.1 M $HNO_3$ solution proved to be the best desorbing agents for the uranyl ions (about 89% recovered in both cases). While the recovery level of both ions is comparable in acidic media, a difference occurs when using a basic desorbing agent ($Na_2CO_3$), in which the uranyl ions are recovered to a higher extent than the thorium ones (89% compared to 58% respectively).

**Table 4**
Desorption results on magnetic chitosan composite particles loaded with radioactive ions.

| Radioactive ion | Desorption in 0.1 M solution (%) | | | |
|---|---|---|---|---|
| | NaCl | $Na_2CO_3$ | HCl | $HNO_3$ |
| $Th^{4+}$ | 66.52 | 58.45 | 82.91 | 87.38 |
| $UO_2^{2+}$ | 77.94 | 89.24 | 80.41 | 88.75 |

## 5. Conclusions

Comparison of the properties before and after metal ion adsorption provides evidence that both sorbates were bound and their distribution on the sorbent surface was uniform. The sorbent saturation magnetization decreased from 24 to 18 emu/g following the adsorption process. This value is still high enough to allow suitable magnetic field separation and recovery of the metal loaded material from the liquid phase.

The optimum parameters for the adsorption process were determined, namely the sorbent mass (0.004 g), the target ion concentration (50 mg/L) and the contact time (120 min). The experimental data were fitted using three models: Langmuir, Freundlich, and respectively Dubinin–Radushkevich isotherm. The results show that the material under study has a superior adsorption capacity for uranyl ions (666.67 mg/g) and respectively a similar one for thorium ions (312.50 mg/g) when compared to other low-cost adsorbents reported in the literature.

The study of the ion partition coefficient versus temperature and evaluation of the thermodynamic parameters associated with the process evidenced that the radiocation adsorption is spontaneous, endothermic and that it is favoured by temperature increase.

Metal desorption studies revealed that both ions may be recovered to the extent of over 80% when using acidic desorbing agents (nitric and hydrochloric acid). Uranyl ions may also desorb to a high recovery level (89%) with the aid of sodium carbonate solutions.

## Acknowledgements

This work was supported by CNCSIS – UEFISCDI, project number PNII-IDEI code 314/2008 (contract 660/2009).

## References


Aamrani, S., Giménez, J., Rovira, M., Seco, F., Grivé, M., Bruno, J., Duro, L. & Pablo, J. (2007). A spectroscopic study of uranium(VI) interaction with magnetite. *Applied Surface Science*, *253*, 8794–8797.

Akkaya, R. & Ulusoy, U. (2008). Adsorptive features of chitosan entrapped in polyacrylamide hydrogel for $Pb^{2+}$, $UO_2^{2+}$, and $Th^{4+}$. *Journal of Hazardous Materials*, *151*, 380–388.

Akperov, E. O., Maharramov, A. M. & Akperov, O. G. (2009). Uranyl ion adsorption using novel cross-linked maleic anhydride–allyl propionate–styrene terpolymer. *Hydrometallurgy*, *100*, 76–81.

Ambashta, R. D. & Sillanpaa, M. (2010). Water purification using magnetic assistance: a review. *Journal of Hazardous Materials*, *180*, 38–49.

Anirudhan, T. S., Rijith, S. & Tharun, A. R. (2010). Adsorptive removal of thorium(IV) from aqueous solutions using poly(methacrylic acid)-grafted chitosan/bentonite composite matrix: Process design and equilibrium studies. *Colloids and Surfaces A: Physicochemical and Engineering Aspects*, *368*, 13–22.

Barakat, M.A., New trends in removing heavy metals from industrial wastewater. Arabian Journal of Chemistry, in press, doi:10.1016/j.arabjc.2010.07.019.

Chen, A. H. & Chen, S. M. (2009). Biosorption of azo dyes from aqueous solution by glutaraldehyde-crosslinked chitosans. *Journal of Hazardous Materials*, *172*, 1111–1121.

Chen, A. H., Liu, S. C., Chen, C. Y. & Chen, C. Y. (2008). Comparative adsorption of Cu(II), Zn(II), and Pb(II) ions in aqueous solution on the crosslinked chitosan with epichlorohydrin. *Journal of Hazardous Materials*, *154*, 184–191.

Crini, G. (2005). Recent developments in polysaccharide-based materials used as adsorbents in wastewater treatment. *Progress in Polymer Science*, *30*, 38–70.

Guerra, D. L., Viana, R. R. & Airoldi, C. (2009). Adsorption of thorium cation on modified clays MTTZ derivative. *Journal of Hazardous Materials*, *168*, 1504–2151.

Hritcu, D., Dodi, G., Silion, M., Popa, N. & Popa, M. I. (2011). Composite magnetic chitosan microspheres: In situ preparation and characterization. *Polymer Bulletin*, *67*, 177–186.

Humelnicu, D., Dinu, M. V. & Dragan, E. S. (2011). Adsorption characteristics of $UO_2^{2+}$ and $Th^{4+}$ ions from simulated radioactive solutions onto chitosan/clinoptilolite sorbents. *Journal of Hazardous Materials*, *185*, 447–455.

Kazya, S. K., D'Souzab, S. F. & Sar, P. (2009). Uranium and thorium sequestration by a *Pseudomonas* sp.: Mechanism and chemical characterization. *Journal of Hazardous Materials*, *163*, 65–72.

Khan, M. H., Ali, A. & Khan, N. N. (2001). Spectrophotometric determination of thorium with disodium salt of Arsenazo III in perchloric acid. *Journal of Radioanalytical and Nuclear Chemistry*, *250*, 353–357.

Kilincarslan, A. & Akyil, S. (2005). Uranium adsorption characteristic and thermodynamic behavior of clinoptilolite zeolite. *Journal of Radioanalytical and Nuclear Chemistry*, *264*, 541–548.

Korichia, S. & Bensmailia, A. (2009). Sorption of uranium (VI) on homoionic sodium smectite experimental study and surface complexation modeling. *Journal of Hazardous Materials*, *169*, 780–793.

Kutahyali, C. & Eral, M. (2010). Sorption studies of uranium and thorium on activated carbon prepared from olive stones: Kinetic and thermodynamic aspects. *Journal of Nuclear Materials*, *396*, 251–256.

Limousin, G., Gaudet, J.-P., Charlet, L., Szenknect, S., Barthes, V. & Krimissa, M. (2007). Sorption isotherms: a review on physical bases, modeling and measurement. *Applied Geochemistry*, *22*, 249–275.

Merroun, M. L., Geipel, G., Nicolai, R., Heise, K.-H. & Selenska-Pobell, S. (2003). Complexation of uranium (VI) by three eco-types of *Acidithiobacillus ferrooxidans* studied using time-resolved laser-induced fluorescence spectroscopy and infrared spectroscopy. *BioMetals*, *16*, 331–339.

Muzzarelli, R. A. A. (2011). Potential of chitin/chitosan-bearing materials for uranium recovery: An interdisciplinary review. *Carbohydrate Polymers*, *84*, 54–63.

Ozmen, M., Can, K., Arslan, G., Tor, A., Cengeloglu, Y. & Ersoz, M. (2010). Adsorption of Cu(II) from aqueous solution by using modified $Fe_3O_4$ magnetic nanoparticles. *Desalination*, *254*, 162–169.

Rojo, I., Seco, F., Rovira, M., Giménez, J., Cervantes, G., Martí, V. & Pablo, J. (2009). Thorium sorption onto magnetite and ferrihydrite in acidic conditions. *Journal of Hazardous Materials*, *385*, 474–478.

Roonasi, P. & Holmgren, A. (2009). An ATR-FTIR study of sulphate sorption on magnetite; rate of adsorption, surface speciation, and effect of calcium ions. *Journal of Colloid and Interface Science*, *333*, 27–32.

Savyvin, S. B. (1961). Analytical Use of arsenazo III determination of thorium, zirconium, uranium and rare earth elements. *Talanta*, *8*, 673–679.

Talip, Z., Eral, M. & Hicsönmez, Ü. (2009). Adsorption of thorium from aqueous solutions by perlite. *Journal of Environmental Radioactivity*, *100*, 139–143.

Wang, J.-s., Peng, R.-t., Yang, J.-h., Liu, Y.-c. & Hu, X.-j. (2011). Preparation of ethylenediamine-modified magnetic chitosan complex for adsorption of uranyl ions. *Carbohydrate Polymers*, *84*, 1169–1175.